



ELSEVIER

Journal of Chromatography A, 853 (1999) 469–477

---

---

JOURNAL OF  
CHROMATOGRAPHY A

---

---

# Interaction of cyclophilin and cyclosporins monitored by affinity capillary electrophoresis

Steffen Kiessig, Holger Bang, Frank Thunecke\*

*Max-Planck Research Division "Enzymology of Protein Folding", Weinbergweg 22, D-06120 Halle/Saale, Germany*

---

## Abstract

The affinity capillary electrophoretic separation of the complex of the enzyme cyclophilin (Cyp) with the immunosuppressive drug cyclosporin A (CsA) from uncomplexed Cyp and CsA in phosphate buffer (pH 8) under non-denaturing conditions by equilibrium-mixture analysis is reported. Using a new approach combining mobility-shift analysis and electrophoretically mediated microanalysis the binding constant of rhCyp18 to CsA and derivatives was estimated. © 1999 Elsevier Science B.V. All rights reserved.

**Keywords:** Affinity capillary electrophoresis; Electrophoretically mediated microanalysis; Cyclophilin; Cyclosporins; Enzymes; Peptides

---

## 1. Introduction

Cyclosporin A (CsA) is a cyclic undecapeptide obtained from fungi and widely used as an immunosuppressive drug to prevent graft rejection following organ transplantation [1]. It binds and competitively inhibits the enzyme cyclophilin (Cyp) a peptidyl-prolyl-*cis/trans*-isomerase (PPIase) in the nanomolar range [2–4]. The Cyp–CsA complex then interacts with other proteins in a way not yet known in detail and probably suppresses T cell proliferation [5]. The therapeutic use of CsA is however hampered by some disadvantages, for example its toxicity and the poor solubility in water. Therefore there is an ongoing search for CsA derivatives with similar efficacy but less toxicity and better solubility.

Capillary electrophoretic methods for the investigation of binding properties are referred to as

affinity capillary electrophoresis (ACE) which is a promising technique to monitor the molecular interaction of biomolecules [6–9]. The affinity can be visualized, if the binding partners and the formed complex exhibit different electrophoretic mobilities. This is however a crucial point. The electrophoretic mobility depends on the charge and the hydrodynamic radius determined by molecular mass and shape. For protein–ligand interactions charged ligands are very favorable because the binding of a small uncharged ligand to a protein causes only a slight change in mass. Further complications arise from the fact that non-denaturing separation conditions are required. This precludes background electrolytes with pH extremes and detergents otherwise quite common for protein separations [10].

In the case of tight-binding systems (slow on–off kinetics) an additional peak for the complex maybe observable using the so-called equilibrium-mixture analysis. Weak-binding complexes (rapid on–off kinetics) are investigated usually by a procedure known as mobility-change analysis [6].

---

\*Corresponding author. Tel.: +49-345-5522-822; fax: +49-345-5511-972.

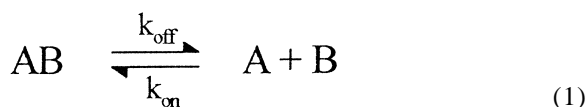
E-mail address: thunecke@enzyme-halle.mpg.de (F. Thunecke)

Electrophoretically mediated microanalysis (EMMA) is a technique using the capillary as a microreactor [11–13]. Different migrating reagents were in a way injected that they pass each other during the electrophoretic run thereby creating a reaction zone followed by the detection of the reaction products.

The aim of this work was to separate the Cyp–CsA complex from free Cyp and to develop a method to monitor interactions of Cyp to CsA derivatives including the estimation of the complex stabilities compared to Cyp–CsA.

## 2. Theory

As published in the literature [6] there are two extremes in affinity capillary electrophoresis: low and high affinity systems. They are characterized by high or low dissociation constants  $K_d$ , respectively. Complex formation and decomposition can be described by Eq. (1) where  $K_d$  is the dissociation constant, AB is the dimeric complex and A and B are complex forming reactants,  $k_{on}$  is the rate constant of the association,  $k_{off}$  is the rate constant of the complex dissociation reaction.



Complex stability is determined by  $K_d$  and characterized by Eq. (2) where  $[A]_{eq}$ ,  $[B]_{eq}$  and  $[AB]_{eq}$  are the concentrations of the reactants in equilibrium,  $[A]_0$  and  $[B]_0$  are the initial concentrations of the reactants.

$$K_d = \frac{k_{off}}{k_{on}} = \frac{[A]_{eq}[B]_{eq}}{[AB]_{eq}} = \frac{([A]_0 - [AB]_{eq})([B]_0 - [AB]_{eq})}{[AB]_{eq}} \quad (2)$$

Rearranging Eq. (2) for  $[AB]$  results in the following Eq. (3) which allows one to determine the concentration of the complex in equilibrium.

$$[AB]_{eq} = \frac{([A]_0 + [B]_0 + K_d)}{2} - \sqrt{\frac{([A]_0 + [B]_0 + K_d)^2}{4} - ([A]_0[B]_0)} \quad (3)$$

Two experimental setups were described in the literature: mobility-change analysis and equilibrium-mixture analysis [6]. While the first type is the method of choice for low affinity systems the second type is applied to high affinity systems. Nevertheless both setups are possible for each of the systems.

## 3. Experimental

### 3.1. Chemicals

All chemicals used were of analytical grade. Water was triple-distilled grade produced by a Milli-Q system (Millipore, Eschborn, Germany). Recombinant human cyclophilin 18 (rhCyp18) from *E. coli* was a gift of J. Rahfeld of our institute. CsA, cyclosporin H (D-<sup>11</sup>MeVal-Cyclosporin, CsH) and biotinylated cyclosporin A (Biotin-LC-PEO-D-<sup>8</sup>Ser-CsA, bCsA) were kindly provided by M. Schutkowski from the synthesis group of our institute. Ac-Ala-Ala was supplied by Bachem (Heidelberg, Germany). KCl, 4-(2-hydroxyethyl)-1-piperazine-ethanesulfonic acid (HEPES), sodium dodecyl sulfate (SDS), NaH<sub>2</sub>PO<sub>4</sub> and Na<sub>2</sub>HPO<sub>4</sub> were obtained from Sigma (Deisenhofen, Germany). Dimethyl sulfoxide (DMSO) was supplied by Roth (Karlsruhe, Germany).

### 3.2. Apparatus

Capillary electrophoresis was performed on 270A-HT from Applied Biosystems (Foster City, CA, USA). Data from the UV detector were monitored and processed by Kontron PC Integrator 3.90 (Kontron Instruments, Milan, Italy).

Fused-silica capillary material was provided by Polymicro Technologies (Phoenix, AZ, USA). UV detection was performed at 200 nm. Capillaries of 80 cm (60 cm to the detection window) × 50 μm I.D. were used. Operation voltage was 30 kV. Injection was performed hydrodynamically by a vacuum of 2.54 p.s.i. (16.9 kPa) for 5 s unless otherwise stated. The capillary thermostating system was kept at 26°C.

### 3.3. Methods

Separation buffers were prepared by diluting stock

solutions of sodium phosphate (200 mM, pH 8.0) to the final concentration. All separations were performed in 50 mM phosphate buffer, pH 8.0 under non-denaturing conditions unless otherwise stated. Prior to use the pH was controlled and the buffer was filtered through a 0.22- $\mu\text{m}$  syringe filter (Roth). Ac-Ala-Ala (200  $\mu\text{M}$  in water) was used as an internal standard for migration time and was injected separately in addition to the sample.

For ACE experiments solutions of rhCyp18 were prepared by diluting the stock solution to the required concentration with HEPES buffer (10 mM HEPES, 200 mM KCl). Stock solutions of CsA and derivatives were prepared in DMSO. Prior to incubation CsA solutions were also diluted with HEPES buffer and mixed with rhCyp18 solutions to give the final concentrations. Incubation was performed at 37°C for 15 min. After incubation the mixture was centrifuged and injected.

For EMMA experiments the solutions were diluted in the same way as for ACE but no preincubation was applied. The samples were injected as single sample zones that become mixed on the capillary. Since CsA is uncharged and rhCyp18 is negatively charged under separation conditions rhCyp18 was injected before CsA. A small buffer plug was injected between the two samples to prevent mixing due to contact of the sample zones. The injection regime was 2 s internal standard, 5 s rhCyp18 (rhCyp18 sample zone), 0.5 s running buffer and 5 s CsA (CsA sample zone).

#### 4. Results and discussion

The dissociation constant  $K_d$  of the investigated system rhCyp18–CsA is well characterized by other methods [14,15] and is known to be in the lower nanomolar range. However it should be mentioned here, that almost all data regarding the Cyp–CsA interaction were derived from the enzymatic activity of Cyp and not from a direct measuring of the binding. Since  $K_d$  is very low a big difference between  $k_{\text{on}}$  and  $k_{\text{off}}$  is present and the system can be described as a tight binding or high affinity system. In addition CsA derivatives with unknown binding properties were investigated. Therefore both modes of ACE were applied.

Unfortunately, in the case of mobility-change

analysis the use of CsA is hampered by the poor solubility of CsA in water. Therefore CsA must be solved in organic solvents like DMSO or ethanol and can be diluted afterwards with buffer up to a limit of about 50  $\mu\text{M}$ . These solvents as additives in the buffer system would probably disturb the native binding properties of rhCyp18 and cause changes in the dissociation constants. Therefore in a new approach the mobility-change analysis mode known from ACE was combined with an EMMA experiment. The contact time is limited to the time when the sample zones pass each other on capillary. But this technique is only applicable to systems with fast complexation kinetics (high  $k_{\text{on}}$  value).

##### 4.1. Equilibrium-mixture analysis

In equilibrium-mixture analysis the reactants are preincubated in a reaction tube and injected in bare separation buffer. In that case complexed and free reactants are separable if the complex is stable and exhibits changed electrophoretic mobility. On the one hand no or less complex decomposition should appear during separation according to a low  $K_d$  value. On the other hand a changed migration behavior of the complex compared to the free reactants is necessary to achieve a separation.

The experimental setup was described in Section 3.3. The concentration of rhCyp18 was kept constant while the concentration of CsA was varied in the range 0 to 25  $\mu\text{M}$ . After incubation the samples were separated in a plain phosphate buffer at pH 8. The background electrolyte was selected after optimization. To assure a non-denaturing environment the pH range is restricted to 5–8.5 and all kinds of detergents should be avoided. Fig. 1 shows the separation of samples with increasing amount of CsA. The rhCyp18 signal disappears with increasing concentration of CsA and another peak assigned to the complex rhCyp18–CsA emerges. This signal enlarges with increasing CsA concentration in the mixture. At stoichiometric ratio the free rhCyp18 is completely transferred into the complex according to the value of  $K_d$ . The concentration of CsA exceeding the rhCyp18 concentration could not be detected because CsA is chargeless and migrates with the electroosmotic flow (EOF). The EOF signal is however dominated by a huge peak caused by the solvent DMSO that overlays the small CsA signal. It

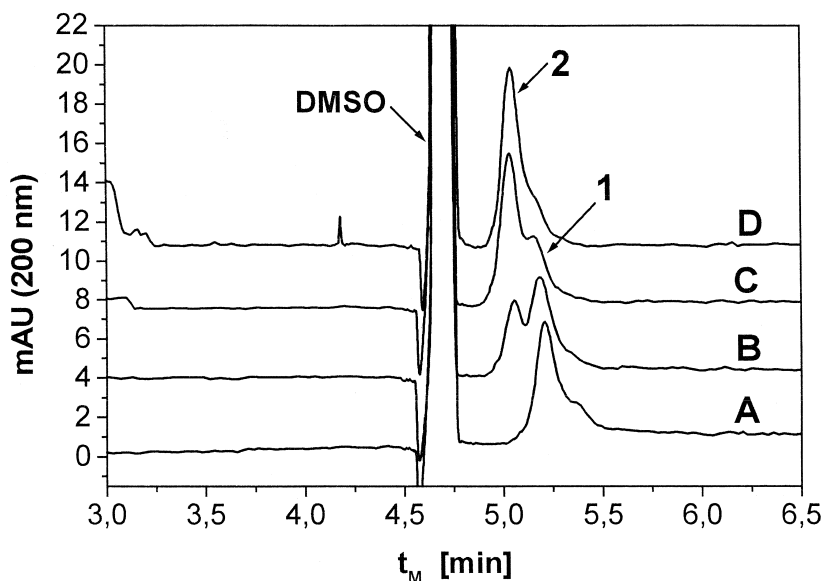


Fig. 1. Separation of rhCyp18 (1) and rhCyp18–CsA complex (2) after preincubation using varying CsA concentrations. 6.1  $\mu\text{M}$  rhCyp18 (A), 6.1  $\mu\text{M}$  rhCyp18 + 2  $\mu\text{M}$  CsA (B), 6.1  $\mu\text{M}$  rhCyp18 + 4  $\mu\text{M}$  CsA (C), 6.1  $\mu\text{M}$  rhCyp18 + 7  $\mu\text{M}$  CsA (D). CE conditions: fused-silica capillary 80 cm  $\times$  50  $\mu\text{m}$  I.D.; temperature, 26°C; voltage, 30 kV; UV detection at 200 nm; separation buffer, 0.05 M phosphate, pH 8.0; hydrodynamic injection, 2/5 s (2.54 p.s.i.) internal standard/sample.

should be noted that the separation is complicated by the fact that complexation does not provide an additional charge and the molecular weight difference of the complexed and uncomplexed species is only about 1000 g/mol at a molecular weight of about 18 000 g/mol for rhCyp18. Furthermore it is noteworthy that the peak of the rhCyp18–CsA complex is narrow and more symmetric in shape than the peak of unbounded rhCyp18. This might be due to restrictions in the conformational flexibility of rhCyp18 when complexed to CsA.

Some additional experiments were made to assure that the emerging peak belongs to the rhCyp18–CsA complex. First the separation conditions were changed. In the presence of SDS in the separation buffer the complex is not stable due to the inclusion of CsA in micelles and the denaturing of rhCyp18. Fig. 2 illustrates the separation of incubated rhCyp18–CsA mixtures under denaturing conditions. Separated peaks for rhCyp18 and CsA were detected. With increasing amounts of CsA in the mixture only the CsA peak changes according to the concentration while the rhCyp18 peak remains constant.

In a next step CsA was substituted by CsH, a derivative of CsA that is known for minimal binding to rhCyp18. Under the same separation conditions stated above in the methods part only the unchanged rhCyp18 peak and no complex peak could be detected with CsH (data not shown).

Although the arising peak is assigned to the complex the experimental setup is difficult regarding the determination of  $K_d$  for rhCyp18–CsA usually done by a Scatchard plot [6,8]. The reagents were employed in micromolar concentrations to enable UV detection whereas the dissociation constant is in the nanomolar range. This divergence of three orders of magnitude causes an almost complete complexation of the CsA in the mixture as long as its concentration is lower than that of rhCyp18. The concentration of the complex increases with the concentration of the added CsA and is nearly the value of the CsA ( $[\text{CsA}] < [\text{rhCyp18}]$ ). When all rhCyp18 is complexed ( $[\text{CsA}] > [\text{rhCyp18}]$ ) free CsA appears in the mixture. This effect can be calculated using Eq. (3). If  $[\text{A}]_0 \approx [\text{B}]_0 \gg K_d$  the influence of  $K_d$  on the concentration of AB is minimal. In that

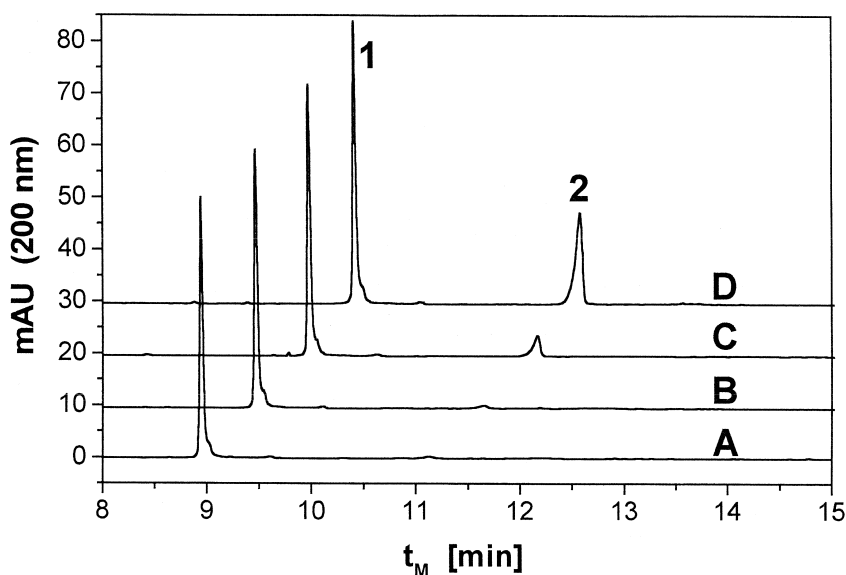


Fig. 2. Separation of preincubated mixture of rhCyp18 (1) and CsA (2) under denaturing conditions. 7.1  $\mu\text{M}$  rhCyp18+1.5  $\mu\text{M}$  CsA (A), 7.1  $\mu\text{M}$  rhCyp18+3  $\mu\text{M}$  CsA (B), 7.1  $\mu\text{M}$  rhCyp18+7.5  $\mu\text{M}$  CsA (C), 7.1  $\mu\text{M}$  rhCyp18+25  $\mu\text{M}$  CsA (D). CE conditions: fused-silica capillary 80 cm $\times$ 50  $\mu\text{m}$  I.D.; temperature, 26°C; voltage, 30 kV; UV detection at 200 nm; separation buffer, 0.1 M borate, pH 8.0+0.03 M SDS; hydrodynamic injection, 5 s (2.54 p.s.i.).

case [AB] is mainly determined by  $[A]_0$  and  $[B]_0$ . Due to this behavior [see also Eq. (2)] estimations of  $K_d$  are hampered by an unacceptable large error. For an error reduction the very small changes in the concentration (or the peak area) must be determined with an accuracy of 0.1%. The slight changes are however dominated by the much higher error of the method (1 to 5%).

But the setup is helpful for controlling the complete complexation of rhCyp18 with CsA under changed experimental conditions like different buffer systems or additives.

Moreover the separation of free and complexed protein allows in a single experiment to decide if a further ligand like calcineurin interacts with the bound rhCyp18, the unbound or both.

Another application is the screening for tight binding CsA derivatives. The separation of incubated mixtures of rhCyp18 with CsA derivatives allows to estimate if the binding constant of the derivative is in the same range as for native CsA, lower or much lower (non-binding).

Therefore a CsA derivative with unknown binding

properties, biotinylated CsA (bCsA), was investigated. Biotinylation is a very common derivatization procedure to fix biomolecules to avidin conjugates on matrices or beads.

Fig. 3 shows the separation of rhCyp18 and rhCyp18–bCsA complex. At stoichiometric concentrations (Fig. 3B) free rhCyp18 can be detected. Even an excess amount of bCsA does not provide a complete complexation of rhCyp18 (Fig. 3C). On the one hand separation of complexed and uncomplexed rhCyp18 shows that rhCyp18–bCsA interaction is characteristic for a high affinity system. On the other hand the incomplete complexation at stoichiometric concentrations is a hint for a decreased complex stability compared to rhCyp18–CsA. Knowing these facts it can be estimated that the  $K_d$  of rhCyp18–bCsA is higher than the  $K_d$  of rhCyp18–CsA but lower than the  $K_d$  of rhCyp18–CsH.

#### 4.2. Electrophoretically mediated microanalysis

Although exact  $K_d$  measurements with EMMA are difficult as well better estimations of  $K_d$  are possible.

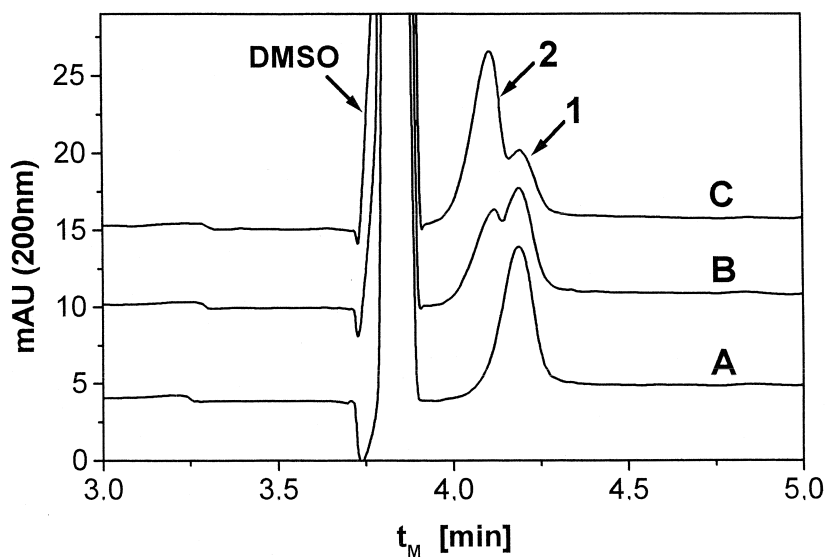


Fig. 3. Separation of rhCyp18 (1) and rhCyp18-bCsA complex (2) after preincubation.  $6.1 \mu\text{M}$  rhCyp18 incubated with  $0 \mu\text{M}$  biotinylated CsA (A),  $6 \mu\text{M}$  biotinylated CsA (B),  $10 \mu\text{M}$  biotinylated CsA (C). CE conditions: separation buffer,  $0.05 \text{ M}$  phosphate, pH 8.0; for other conditions see Fig. 2.

Microanalysis was applied on the formation of the complex on capillary. Samples of rhCyp18 and CsA or derivatives were injected separately without mixing or incubating. The formation of the rhCyp18-CsA complex takes place on capillary when the sample zones pass each other. The injection order of the samples is very important in these experiments. From equilibrium-mixture analysis was known that rhCyp18 has a higher migration time or a lower observed mobility than CsA. For that reason rhCyp18 is injected before CsA to provide mixing of the sample zones on capillary. This experimental setup is advantageous because the necessary amount of rhCyp18 is decreased tremendously. For a rapid screening EMMA is the method of choice because no sample mixing and incubation in a batch is required. As already stated above the method is only suitable for systems with high  $k_{\text{on}}$  rates. In that case even a short mixing time can provide a measurable effect in peak shape or migration behavior.

Fig. 4 shows electropherograms where the concentration of rhCyp18 was kept at  $6.1 \mu\text{M}$  whereas the concentration of CsA was varied in a range of 0 to  $20 \mu\text{M}$  while the length of the sample zones were constant in both cases. With increasing concentration of CsA peak shape and migration time of peak 1

were changed. Peak 1 shifted continuously from the migration time of the uncomplexed rhCyp18 to the value of the complex. This change in mobility was used to visualize complex formation.

To assure that the minute shift in migration is caused by complex formation in a second approach the concentration of rhCyp18 was varied whereas the concentration of CsA was kept constant at  $6 \mu\text{M}$ . In that case all injected rhCyp18 is complexed completely up to a concentration of  $6 \mu\text{M}$  for rhCyp18. As expected only one steadily increasing peak with the migration time of the complex (Fig. 5  $\nabla$ ) was observed.

Fig. 5 further demonstrates the dependence of the mobility of peak 1 in Fig. 4 on the amount of CsA ( $\blacksquare$ ) in the sample zone. The mobility difference was calculated using the internal standard Ac-Ala-Ala to correct the influence of small changes in viscosity or temperature on migration time since the measured effect on the mobility is very small. The mobility difference increases linearly up to  $6 \mu\text{M}$  and remains constant afterwards. At  $6 \mu\text{M}$  all rhCyp18 is complexed by CsA. Additional CsA cannot change the mobility anymore.

These mobility-change experiments using EMMA were applied to other CsA derivatives as well.

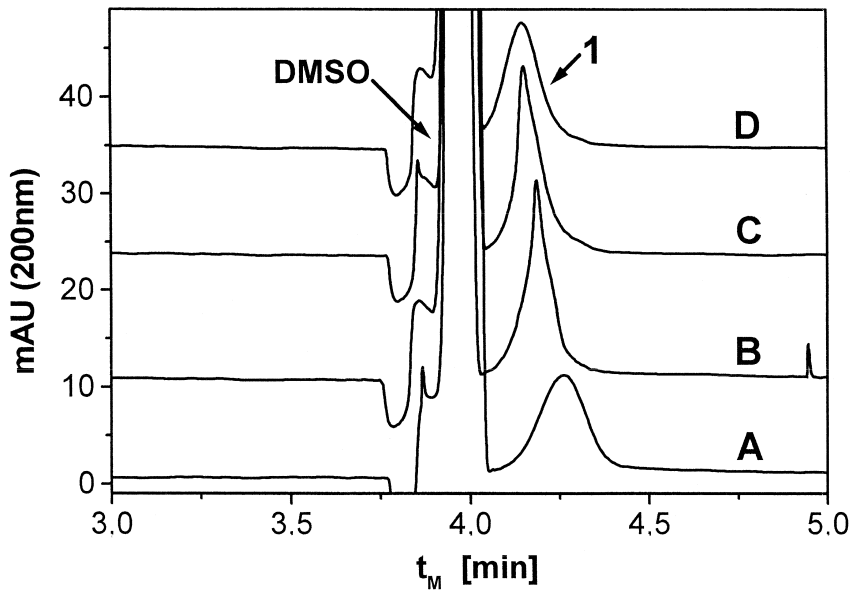


Fig. 4. EMMA experiment with rhCyp18 (1) and varying CsA concentrations. 0  $\mu\text{M}$  CsA in CsA sample zone (A), 3  $\mu\text{M}$  CsA in CsA sample zone (B), 6  $\mu\text{M}$  CsA in CsA sample zone (C), 10  $\mu\text{M}$  CsA in CsA sample zone (D). Conditions: 6.1  $\mu\text{M}$  rhCyp18; hydrodynamic injection at 2.54 p.s.i., 2 s internal standard, 5 s rhCyp18, 0.5 s buffer, 5 s CsA, for other conditions see Fig. 3.

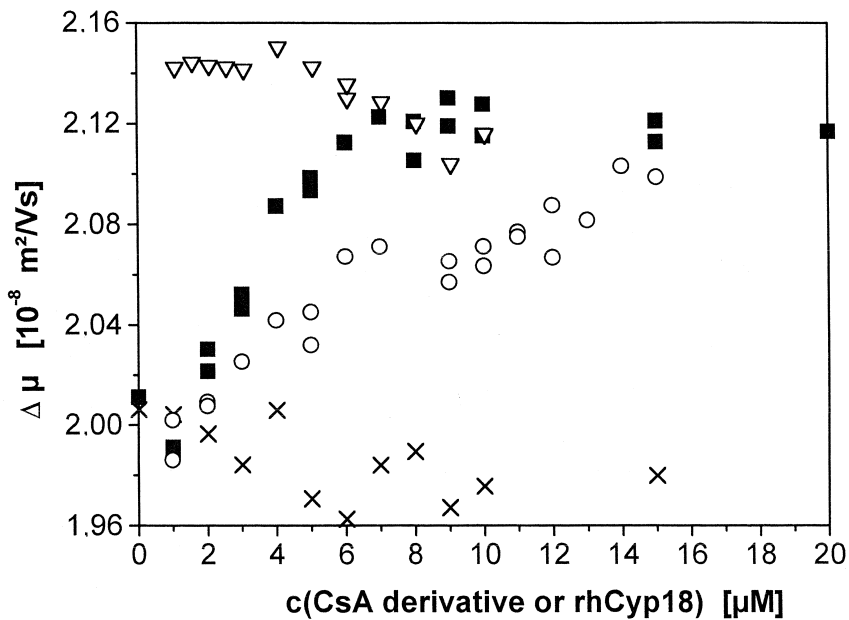


Fig. 5. Dependence of mobility difference between rhCyp18 and internal standard on CsA derivative concentration using EMMA. 6.1  $\mu\text{M}$  rhCyp18 constant: CsA (■), biotinylated CsA (○), CsH (×); 6  $\mu\text{M}$  CsA constant: rhCyp18 (▽).

In the case of CsH ( $\times$ ) no mobility shift was observed. This was expected because of the known poor binding properties to rhCyp18.

The mobility shift in presence of bCsA ( $\circ$ ) is also different compared with native CsA. The maximum shift is reached at bCsA concentrations of about 14  $\mu\text{M}$ . The results are in good agreement with the equilibrium-mixture experiments where also an excess of bCsA was required to achieve a complete complexation of rhCyp18.

The data of Fig. 5 were used for a rough estimation of  $K_d$  for CsA and bCsA (Fig. 6). The methods to estimate binding constants from mobility-change analysis described in the literature [6,8,16] based on the assumption that the concentration of the binding partner mixed to the buffer is constant over the whole capillary. But this is not the case in our approach combining mobility-change analysis with EMMA. Measured mobility differences were compared with simulated data. The simulation was done using Eq. (3). It is difficult to fit an accurate curve on the data points between the straight and the dashed line. These lines cover two-orders of magnitude, but minute changes in the measured data cause a large

effect on the estimated  $K_d$ . The necessary accuracy in the measurement of  $\Delta\mu$  especially in the region of stoichiometric ratio to provide an exact determination of  $K_d$  cannot be achieved. As pointed out above the problem is again the big difference between  $K_d$  and the reagent concentrations used.

Using the simulated curves in Fig. 6 it is possible to estimate the  $K_d$  values for CsA and bCsA as in the range of 10 to 100 nM and 1 to 4  $\mu\text{M}$ , respectively. The value for native CsA is one-order of magnitude higher compared with the constants published in the literature [4]. However it is known that the  $K_d$  especially depends on experimental conditions like mixing time and solvents used. For short mixing times as provided by EMMA higher  $K_d$  values are published than for equilibrated solutions [17].

Under these experimental conditions the dissociation constant for bCsA is two-orders of magnitude higher than that of CsA. The error of the estimated  $K_d$  value is in the same range as known from other methods used to determine binding constants [4]. However the  $K_d$  value for bCsA has to be confirmed by independent methods under identical experimental conditions.

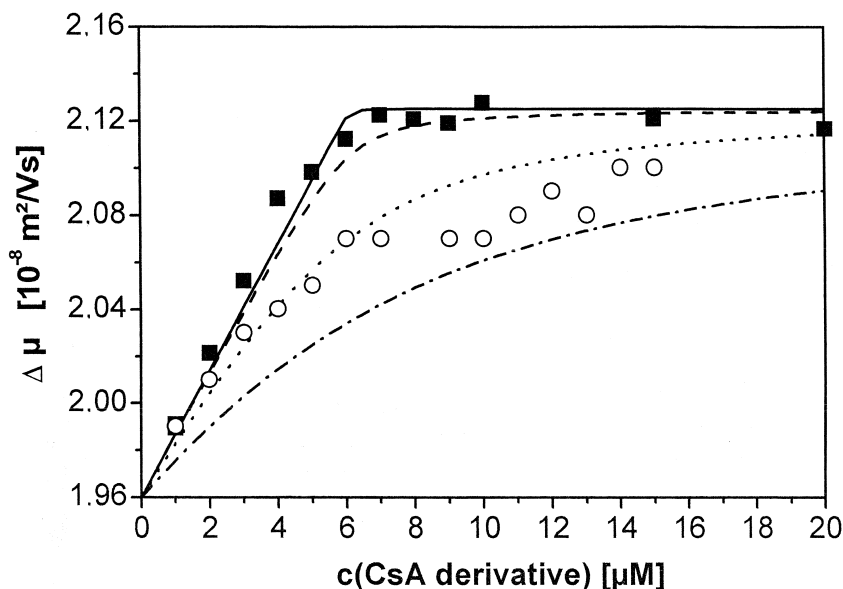


Fig. 6. Estimation of binding constants for rhCyp18–CsA and –bCsA by comparing obtained EMMA data for mobility differences with curves simulated according to Eq. (3) for assumed  $K_d$  values. CsA ( $\blacksquare$ ), biotinylated CsA ( $\circ$ ),  $K_d=1$  nM (straight line),  $K_d=100$  nM (dashed line),  $K_d=1$   $\mu\text{M}$  (dotted line),  $K_d=4$   $\mu\text{M}$  (dashed dotted line).



## 5. Conclusions

The results demonstrate that ACE in the equilibrium-mixture analysis mode and EMMA provide a simple and effective system for the estimation of binding constants for rhCyp18 and CsA and derivatives. The order of magnitude and a comparison of dissociation constants for CsA derivatives can be achieved in a short time with minimal consumption of substances. This is important for the study of the influence of derivatization of the CsA molecule or Cyp mutants on the Cyp–CsA binding properties. Furthermore the degree of complexation under the chosen experimental conditions (buffers, salts, other organic solvents) can be monitored. The visualization of the rhCyp18–CsA complex separated from uncomplexed Cyp also offers the opportunity to study further interactions of the complex to other proteins like calcineurin and may allow to distinguish if partners interact with the complexed or uncomplexed Cyp or both. Finally these experimental setups seem transferable to other high affinity systems, e.g., other PPIases and inhibitors.

## Acknowledgements

This work was supported by grants from the Boehringer-Ingelheim Foundation. F.Th. thanks the state of Saxony-Anhalt for providing a habilitation scholarship.

## References

- [1] J.F. Borel, C. Feurer, H.U. Gubler, H. Stahelin, *Agents Actions* 43 (1994) 179.
- [2] G. Fischer, B. Wittmann-Liebold, K. Lang, T. Kiefhaber, F.X. Schmid, *Nature* 337 (1989) 476.
- [3] N. Takahashi, T. Hayano, M. Suzuki, *Nature* 337 (1989) 473.
- [4] G. Fischer, *Angew. Chem., Int. Ed. Engl.* 33 (1994) 1415.
- [5] B.D. Kahan, *New Engl. J. Med.* 321 (1989) 1725.
- [6] K. Shimura, K. Kasai, *Anal. Biochem.* 251 (1997) 1.
- [7] G. Rippel, H. Corstjens, H.A.H. Billiet, J. Frank, *Electrophoresis* 18 (1997) 2175.
- [8] Y.H. Chu, W.J. Lees, A. Stassinopoulos, C.T. Walsh, *Biochemistry* 33 (1994) 10616.
- [9] L. Tao, R.T. Kennedy, *Electrophoresis* 18 (1997) 112.
- [10] V. Dolnik, *Electrophoresis* 18 (1997) 2353.
- [11] F.E. Regnier, D.H. Patterson, B.J. Harmon, *Trends Anal. Chem.* 14 (1995) 177.
- [12] L.Z. Avila, G.M. Whitesides, *J. Org. Chem.* 58 (1993) 5508.
- [13] D.H. Patterson, B.J. Harmon, F.E. Regnier, *J. Chromatogr. A* 662 (1994) 389.
- [14] M.A. Levy, M. Brandt, G.P. Livi, D.J. Bergsma, *Transplant. Proc.* 23 (1991) 319.
- [15] T.F. Holzman, D.A. Egan, R. Edalji, R.L. Simmer, R. Helfrich, A. Taylor, N.S. Burres, *J. Biol. Chem.* 266 (1991) 2474.
- [16] K.L. Rundlett, D.W. Armstrong, *Electrophoresis* 18 (1997) 2194.
- [17] B. Janowski, G. Fischer, *Bioorg. Med. Chem.* 5 (1997) 179.